J|A|C|S ARTICLES

Published on Web 08/23/2010

Pressure-Induced Decomposition of Indium Hydroxide

Aleksander Gurlo,* Dmytro Dzivenko, Miria Andrade, Ralf Riedel, Stefan Lauterbach, and Hans-Joachim Kleebe

Fachbereich Material- und Geowissenschaften, Technische Universität Darmstadt, Petersenstr. 23, 64287 Darmstadt, Germany

Received May 18, 2010; E-mail: gurlo@materials.tu-darmstadt.de.

Abstract: A static pressure-induced decomposition of indium hydroxide into metallic indium that takes place at ambient temperature is reported. The lattice parameter of c-$In(OH)_3$ decreased upon compression from 7.977(2) to ~7.45 Å at 34 GPa, corresponding to a decrease in specific volume of ~18%. Fitting the second-order Birch−Murnaghan equation of state to the obtained compression data gave a bulk modulus of 99 ± 3 GPa for c-$In(OH)_3$. The c-$In(OH)_3$ crystals with a size of ~100 nm are comminuted upon compression, as indicated by the grain-size reduction reflected in broadening of the diffraction reflections and the appearance of smaller (~5 nm) incoherently oriented domains in TEM. The rapid decompression of compressed c-$In(OH)_3$ leads to partial decomposition of indium hydroxide into metallic indium, mainly as a result of localized stress gradients caused by relaxation of the highly disordered indium sublattice in indium hydroxide. This partial decomposition of indium hydroxide into metallic indium is irreversible, as confirmed by angle-dispersive X-ray diffraction, transmission electron microscopy imaging, Raman scattering, and FTIR spectroscopy. Recovered c-$In(OH)_3$ samples become completely black and nontransparent and show typical features of metals, i.e., a falling absorption in the 100−250 cm^{-1} region accompanied by a featureless spectrum in the 250−2500 cm^{-1} region in the Raman spectrum and Drude-like absorption of free electrons in the region of 4000−8000 cm^{-1} in the FTIR spectrum. These features were not observed in the initial c-$In(OH)_3$, which is a typical white wide-band-gap semiconductor.

Introduction

The high-pressure behavior of indium oxide (In_2O_3), indium hydroxide [$In(OH)_3$], and indium oxohydroxide (InOOH) has recently gained particular attention, as indicated by a number of density functional theory computational studies as well as experimental high-pressure studies.[1−12] The interest in indium-based materials is due to their technological utilization. Indeed, In_2O_3 is a transparent n-type semiconductor with diverse applications. For example, (i) Sn-doped In_2O_3, known as indium tin oxide (ITO), is the key technological material for solar energy utilization;[13] (ii) Cr^{3+}, Mn^{3+}, and Fe^{3+} -doped In_2O_3 are room-temperature ferromagnetics;[14,15] and (iii) In_2O_3-based gas sensors show high sensitivities to toxic and explosive gases at low temperatures, allowing their application as gas detectors on flexible electronic platforms.[16,17] InOOH and $In(OH)_3$ are wide-band-gap semiconductors that show photocatalytic activity and switchable surface wettability.[18,19] Despite progress in theoretical prediction as well as experimental realization of new polymorphs, a complete pressure−temperature diagram of indium oxide is still lacking. Even less is known about the high-pressure behavior of indium hydroxide and indium oxohydroxide. c-$In(OH)_3$ has the so-called A-site-deficient hydroxyl-perovskite structure [space group $Im\bar{3}$ (No. 204), $a = 7.979$ Å, $Z = 8$].[20] o-InOOH has a disordered rutile structure [space group $P2_1nm$ (No. 31), $a = 5.26$ Å, $b = 4.56$ Å, $c = 3.27$ Å, $Z = 2$] and is an important representative structure type for several oxohydroxides (e.g., high-pressure polymorphs of oxohydrox-

(1) Caracas, R.; Cohen, R. E. *Phys. Rev. B* **2007**, *76*, 184101.
(2) Yusa, H.; Tsuchiya, T.; Sata, N.; Ohishi, Y. *Phys. Rev. B* **2008**, *77*, 064107.
(3) Yusa, H.; Tsuchiya, T.; Tsuchiya, J.; Sata, N.; Ohishi, Y. *Phys. Rev. B* **2008**, *78*, 092107.
(4) Gurlo, A.; Kroll, P.; Riedel, R. *Chem.−Eur. J.* **2008**, *14*, 3306.
(5) Karazhanov, S. Z.; Ravindran, P.; Vajeeston, P.; Ulyashin, A.; Finstad, T. G.; Fjellvag, H. *Phys. Rev. B* **2007**, *76*, 075129.
(6) Tsuchiya, J.; Tsuchiya, T.; Sano, A.; Ohtani, E. *J. Miner. Petrol. Sci.* **2008**, *103*, 116.
(7) Liu, D.; Lei, W. W.; Zou, B.; Yu, S. D.; Hao, J.; Wang, K.; Liu, B. B.; Cui, Q. L.; Zou, G. T. *J. Appl. Phys.* **2008**, *104*, 083506.
(8) Saitoh, H.; Utsumi, W.; Aoki, K. *J. Cryst. Growth* **2008**, *310*, 2295.
(9) Gurlo, A.; Dzivenko, D.; Kroll, P.; Riedel, R. *Phys. Status Solidi RRL* **2008**, *2*, 269.
(10) Xue, X.; Kanzaki, M. *J. Phys. Chem. B* **2007**, *111*, 13156.
(11) Walsh, A.; Catlow, C. R. A.; Sokol, A. A.; Woodley, S. M. *Chem. Mater.* **2009**, *21*, 4962.
(12) Moller, A.; Schmidt, P.; Wilkening, M. *Nachr. Chem.* **2009**, *57*, 239.
(13) Granqvist, C. G. *Sol. Energy Mater. Sol. Cells* **2007**, *91*, 1529.
(14) Philip, J.; Punnoose, A.; Kim, B. I.; Reddy, K. M.; Layne, S.; Holmes, J. O.; Satpati, B.; Leclair, P. R.; Santos, T. S.; Moodera, J. S. *Nat. Mater.* **2006**, *5*, 298.
(15) Gurlo, A.; Ivanovskaya, M.; Barsan, N.; Weimar, U. *Inorg. Chem. Commun.* **2003**, *6*, 569.
(16) Graf, M.; Gurlo, A.; Barsan, N.; Weimar, U.; Hierlemann, A. *J. Nanopart. Res.* **2006**, *8*, 823.
(17) Sahm, T.; Gurlo, A.; Barsan, N.; Weimar, U. *Particul. Sci. Technol.* **2006**, *24*, 441.
(18) Li, Z. H.; Xie, Z. P.; Zhang, Y. F.; Wu, L.; Wang, X. X.; Fu, X. Z. *J. Phys. Chem. C* **2007**, *111*, 18348.
(19) Zhu, W. Q.; Zhai, J.; Sun, Z. W.; Jiang, L. *J. Phys. Chem. C* **2008**, *112*, 8338.
(20) Hyde, B. G.; Andersson, S. *Inorganic Crystal Structures*; Wiley: New York, 1989.

10.1021/ja104278p

ides of iron, aluminum, and gallium[10,21−23]). As found recently, c-$In(OH)_3$ decomposes into o-InOOH at ∼0.1 GPa and 350 °C[10] and at 4 GPa upon heating to 600 °C.[24] o-InOOH forms a pyrite-type structure at ∼14 GPa and ∼1600 °C that is partially transformed into disordered rutile-type InOOH upon decompression.[6,24]

In this communication, decomposition of indium hydroxide induced by a static pressure at ambient temperature is reported. It is shown that this unique process is initiated by rapid decompression, is irreversible, and seems to be intimately related to the disordering of the indium sublattice in indium hydroxide. The compression behavior of c-$In(OH)_3$ was investigated by means of in situ high-pressure X-ray diffraction (XRD) combined with synchrotron radiation. The starting c-$In(OH)_3$ polycrystalline powder, which consisted of cube-shaped crystals with {100} morphology with sizes of ∼100 nm, was compressed in a diamond anvil cell (DAC) at room temperature. As recently reported,[25] this c-$In(OH)_3$ material with {100} morphology decomposes irreversibly to bixbyite-type c-In_2O_3 without formation of any intermediates upon heating to ∼300 °C in air under ambient-pressure conditions. The dehydroxylation of c-$In(OH)_3$ is accompanied by the fragmentation of c-$In(OH)_3$ cube-shaped crystals and can be easily followed even visually, since c-$In(OH)_3$ is white and c-In_2O_3 is yellow in color.

Materials and Methods

Synthesis. The synthesis of c-$In(OH)_3$ cubic-shaped nanocrystals having {100} morphology and sizes of 50−100 nm was performed as follows: (i) dissolution of indium nitrate hydrate (Sigma-Aldrich) in anhydrous ethanol (Rotipuran, 99.8% p.a., CarlRoth); (ii) precipitation of $In(OH)_3$ by 32 wt. % NH_3 solution in water; (iii) washing of the precipitate with water to remove residual solvents and side ions (Na^+, NH_4^+, NO_3^-); and (iv) drying at 115 °C for 10 h in air.[26] To improve the crystallinity of the $In(OH)_3$, the as-synthesized powder was treated at 200 °C and ∼50 kbar (5 MPa) for 10 h in a Teflon-lined autoclave.

In Situ High-Pressure X-ray Diffraction Experiments. High-pressure XRD was performed using a DAC with anvils having flat culets with diameters of 400 μm. The sample powder and a piece of platinum foil (which served as a pressure standard) were loaded into a hole in the preindented rhenium gasket without any pressure medium. The pressure was determined from the equation of state of platinum.[27] The specific volumes of platinum and the sample material at high pressures were derived from energy-dispersive XRD patterns measured using polychromatic synchrotron radiation on beamline F3 at the HASYLAB (DESY, Hamburg). The diffraction patterns were collected at the diffraction angle $2\theta = 8.3°$ in the energy range from 13 to 62 keV using a Ge detector (IGP-25, Princeton Gamma-Tech). Optical microscopy images were taken in reflection and transmission modes in DACs using a common digital camera and a microscope.

Angle-Dispersive Powder X-ray Diffraction Experiments. Angle-dispersive powder XRD of the recovered reddish sample was measured using monochromatic synchrotron radiation with wavelength $\lambda = 0.3654$ Å on beamline ID09A (ESRF, Grenoble). The XRD data were collected with an online image-plate detector. To avoid diffraction from the gasket and platinum foil, the X-ray beam was collimated to about 10 μm × 10 μm.

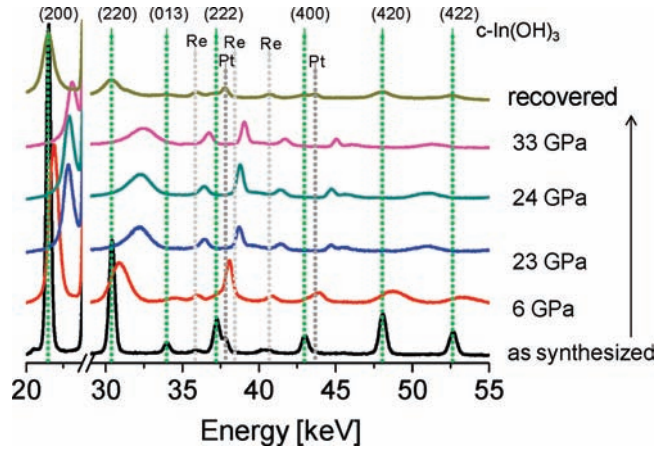

Figure 1. First experiment: in situ energy-dispersive XRD patterns of c-$In(OH)_3$ in a DAC at different pressures. The label "as synthesized" indicates the starting c-$In(OH)_3$ in the DAC at ambient pressure. Tick marks indicate diffraction reflections of c-$In(OH)_3$ (PCPDFWIN 85-1338), Re (PCPDFWIN 89-2935), and Pt (PCPDFWIN 88-2343). The horizontal axis is broken to cut off the indium emission lines (^{49}In Kα_{1-2}, Kβ_{1-3}). At the top, the (*hkl*) planes of c-$In(OH)_3$ are indicated.

TEM Imaging. Transmission electron microscopy (TEM) was performed using an FEI CM20 microscope (Eindhoven, The Netherlands). To prepare the sample for TEM characterization, the material recovered from the DAC experiment was suspended in a droplet of pure ethanol. The droplet was carefully transferred to a holey carbon grid and allowed to dry. The grid was lightly coated with carbon to avoid charging under the electron beam.

Raman and FTIR Spectra. Raman and FTIR spectra were recorded on samples loaded in Re gaskets on a LabRAM Raman HR microscope (Horiba Jobin Yvon) using a 488 nm laser and a 670 FTIR spectrometer (Varian), respectively.

Results and Discussion

Upon slow compression to 33 GPa at room temperature, neither phase transitions nor decomposition of c-$In(OH)_3$ but only a continuous shift and broadening of the c-$In(OH)_3$ reflections were observed (Figure 1). As reported above, under high-temperature conditions, c-$In(OH)_3$ is metastable at pressures above 4 GPa and decomposes into o-InOOH.[24]

The broadening of the c-$In(OH)_3$ reflections could be attributed to either nonhydrostatic stresses in the compressed sample or partial disordering of the crystal structure of indium hydroxide. The former is less probable, as a uniform decrease of dissimilar d_{hkl} with no discontinuities in the interplanar spacings for indium hydroxide and the presence of narrow Pt reflections were observed (Figure 2).

The lattice parameter of c-$In(OH)_3$ decreased upon compression from 7.977(2) Å to ∼7.45 Å at 33 GPa, corresponding to a decrease in specific volume of ∼18%. Fitting the second-order Birch−Murnaghan equation of state[28] to the obtained compression data [$V(P)$] gave a bulk modulus of 99 ± 3 GPa for c-$In(OH)_3$. During further compression slightly above 33 GPa, one of the diamond anvils cracked,[29] which resulted in rapid decompression of the c-$In(OH)_3$ sample to ambient pressure. The decompressed sample was found to have a reddish

(21) Nikolaev, N. A.; Lityagina, L. M.; Dyuzheva, T. I.; Kulikova, L. F.; Bendeliani, N. A. *J. Alloys Compd.* **2008**, *459*, 95.
(22) Bolotina, N. B.; Molchanov, V. N.; Dyuzheva, T. I.; Lityagina, L. M.; Bendeliani, N. A. *Crystallogr. Rep.* **2008**, *53*, 960.
(23) Komatsu, K.; Kuribayashi, T.; Kudoh, Y.; Kagi, H. *Z. Kristallogr.* **2007**, *222*, 1.
(24) Sano, A.; Yagi, T.; Okada, T.; Gotou, H.; Ohtani, E.; Tsuchiya, J.; Kikegawa, T. *J. Miner. Petrol. Sci.* **2008**, *103*, 152.
(25) Schlicker, L.; Riedel, R.; Gurlo, A. *Nanotechnology* **2009**, *20*, 495702.
(26) Gurlo, A.; Miehe, G.; Riedel, R. *Chem. Commun.* **2009**, 2747.
(27) Dewaele, A.; Loubeyre, P.; Mezouar, M. *Phys. Rev. B* **2004**, *70*, 094112.
(28) Birch, F. *J. Geophys. Res.* **1978**, 1257.
(29) The exact pressure at which the anvil cracked was not determined. It can be very roughly estimated to exceed the pressure at the final recorded point by a few gigapascals.

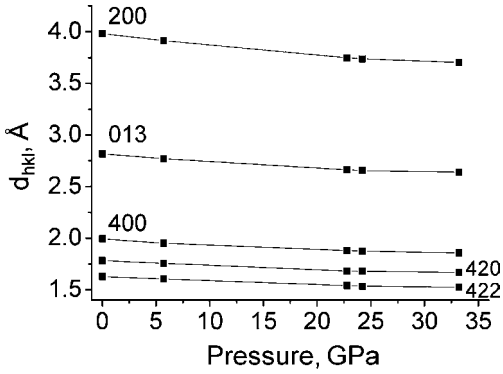

Figure 2. First experiment: interplanar spacing (d_{hkl}) of c-$In(OH)_3$ as a function of pressure.

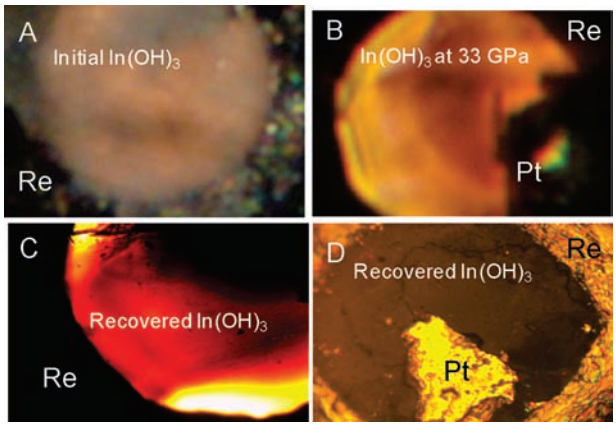

Figure 3. Optical microscopy images of c-$In(OH)_3$ samples loaded in DACs (Re gasket with Pt foil): (A) initial sample (white) at ambient pressure; (B) sample after compression to 33 GPa; (C) sample after rapid decompression to ambient pressure from the first compression experiment; (D) sample recovered to ambient pressure after two successive loadings from the second experiment (see the text). Images A−C were taken under transmitted light and image D under reflected light.

color, in contrast to the white transparent starting material (Figure 3C). Subsequent angle-dispersive XRD analysis revealed the presence of new, less intense reflections corresponding to *d* values of 2.72, 2.46, and 1.68 Å. These reflections can be attributed to the (011), (002), and (112) reflections of metallic indium [space group *I*4/*mmm* (No. 139), $a = 3.292$ Å, $c = 4.87$ Å, $Z = 2$] (Figure 4). The fraction of metallic indium was ~1.5%.

To confirm the possible decomposition of indium hydroxide resulting in nucleation of metallic indium, an additional experiment (hereafter called the second experiment) was performed. The c-$In(OH)_3$ sample was compressed in a DAC to ~20 GPa and quickly decompressed to ambient pressure (Figure 5). During subsequent compression of the same sample to ~34 GPa, significant broadening of the c-$In(OH)_3$ reflections accompanied by continuous darkening of the material was observed. The material became completely black and nontransparent at the maximum pressure (34 GPa). After recovery to ambient pressure, the sample remained black (Figure 3D) and revealed a distinct diffraction reflection at $d = 2.72$ Å (Figure 6b); this finding indicated an increase in the amount of indium in comparison with that after the first rapid decompression (Figure 6c).

The recovered "black" and "red" samples show typical features of metals, namely, a falling absorption in the 100−250 cm^{-1} region accompanied by a featureless spectrum in the

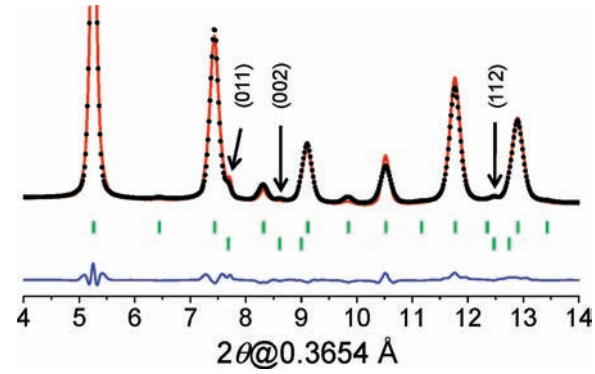

Figure 4. First experiment: Two-phase Rietveld refinement of the "red" c-$In(OH)_3$ sample compressed to ~33 GPa and recovered to ambient conditions with c-$In(OH)_3$ [space group $Im\bar{3}$ (No. 204), $a = 7.970(1)$ Å; upper ticks] and t-In [space group *I*4/*mmm* (No. 139), $a = 3.292(4)$ Å, $c = 4.87(1)$ Å; lower ticks] structures. Solid circles and solid lines indicate observed and calculated intensities, respectively. The difference curve is given at the bottom of the figure. In the top trace, the (*hkl*) planes of t-In are indicated.

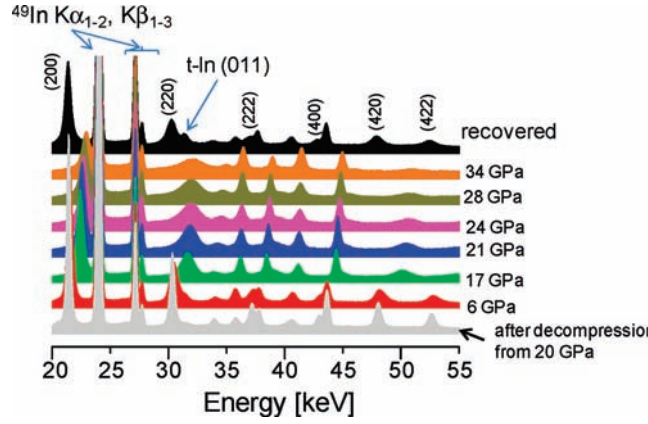

Figure 5. Second experiment: in situ energy-dispersive XRD patterns of c-$In(OH)_3$ that was compressed in a DAC to ~20 GPa and quickly decompressed to ambient pressure. The bottom pattern (labelled as "after decompression from 20 GPa) is for the sample in the DAC at ambient pressure. The next six patterns are for samples compressed to pressures in the range 6−34 GPa (as indicated), and the top pattern is for the sample recovered to ambient pressure after compression up to 34 GPa. For the assignment of diffraction reflections, see Figure 1. In the top pattern, the (*hkl*) planes of c-$In(OH)_3$ and a (011) plane of t-In are indicated.

250−2500 cm^{-1} region in the Raman spectra (Figure 7A) and Drude-like absorption of free electrons in the 4000−8000 cm^{-1} region of the IR spectra (Figure 7B). These features were not observed for the initial c-$In(OH)_3$, which is a typical white wide-band-gap semiconductor.

All of these findings indicate the partial decomposition of indium hydroxide to metallic indium. Hence, the blackening of the recovered samples and their Raman scattering and FTIR spectra confirm the metalization of the recovered c-$In(OH)_3$ samples. Recently, the metalization of nonstoichiometric amorphous gallium oxide accompanied by an insulator to metal transition was shown to be due to an increased nonstoichiometry in amorphous $GaO_{1.2}$ due to the crystallization of stoichiometric Ga_2O_3.[31] In our case, the metalization of c-$In(OH)_3$ is due to the spontaneous nucleation and crystallization of highly dispersed metallic indium in the insulating c-$In(OH)_3$ matrix and

(30) Yang, J.; Frost, R. L.; Martens, W. N. *J. Therm. Anal. Calorim.* **2010**, *100*, 109.

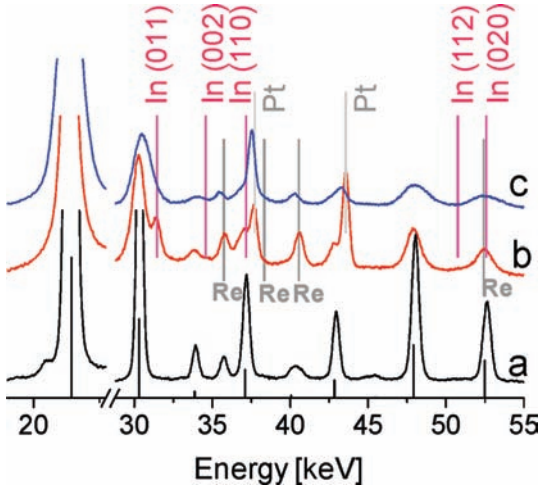

Figure 6. Energy-dispersive XRD patterns of c-In(OH)$_3$ in a DAC at ambient pressure: (a) initial sample; (b) black sample recovered after the second experiment; (c) reddish sample recovered after the first experiment. At the bottom of the figure, the diffraction pattern of c-In(OH)$_3$ (PCPDFWIN 85-1338) is shown. At the top, the diffraction patterns (intensity set to 100% for all reflections) of metallic In (PCPDFWIN 85-1409), metallic Re (PCPDFWIN 89-2935), and Pt (PCPDFWIN 88-2343) are shown.

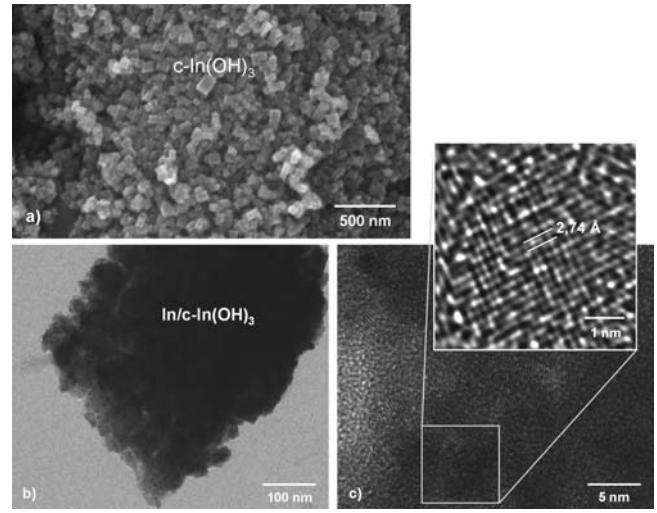

Figure 8. (a) Scanning electron microscopy image of the initial white c-In(OH)$_3$ sample. (b, c) TEM micrographs of the recovered black In/c-In(OH)$_3$ sample. The inset in (c) reveals an inverse FFT image of the boxed region. The measured distance obtained from the inverse FFT image is 2.74 Å, which is in good agreement with the d_{011} distance in t-In.

results from c-In(OH)$_3$ decomposition during the decompression. c-In(OH)$_3$ crystals with sizes of ~100 nm are comminuted upon compression, as indicated by the grain-size reduction reflected in the broadening of the diffraction reflections and the appearance of smaller (~5 nm) incoherently oriented domains, as shown in the TEM images given in Figure 8. The inset of Figure 8C shows an enlarged inverse FFT image of the region marked by the box, which illustrates the small size of the incoherent domains formed upon decompression. The measured distance between bright rows in the inset is 2.74 Å, which corresponds well to the d_{011} value of 2.72 Å in t-In, confirming the formation of indium nanocrystals in the recovered In(OH)$_3$ samples.

The question arises about the origin and mechanism of the c-In(OH)$_3$ decomposition upon decompression. Indium hydroxide can be regarded as having a collapsed A-site-deficient perovskite structure A′A″B$_4$X$_{12}$ (where the A′ and A″ positions are empty and the B and X positions are occupied by indium and oxygen, respectively).[20] In this A-site-deficient hydroxyl-perovskite, the InO$_6$ octahedra are linked with each other by corner (vertex) sharing through O−H···O hydrogen bonding along the edges of the "square" array of oxygen positions coordinating the empty A″ sites. According to the special reflection conditions for diffraction of crystals by radiation, indium atoms (with high scattering power) located in the special

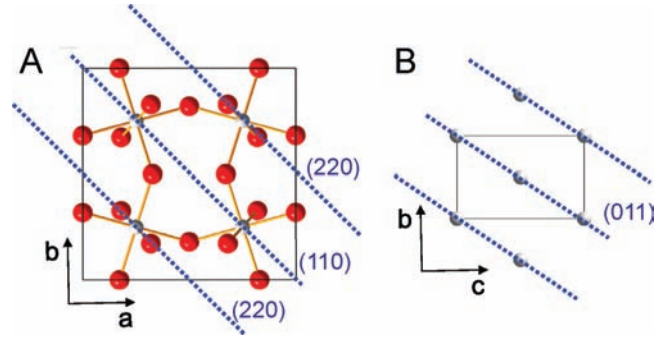

Figure 9. (A) Coordination of indium atoms (small gray circles) by oxygen (large red circles) and interconnection (sharing) of [InO$_6$] octahedra in the c-In(OH)$_3$ structure under ambient-pressure conditions. The {220} planes composed of In atoms are also shown. (B) {011} planes in tetragonal indium.

Wyckoff position ($^1/_4$, $^1/_4$, $^1/_4$; 8c position of space group $Im\bar{3}$) contribute to the set of (hkl; k, $l = 2n$) reflections.[32] The larger broadening of the set of (220) and (420) reflections relative to the others (see Figure 1) most probably indicates a larger disordering of the indium sublattice in comparison with the oxygen sublattice (Figure 9). Recently, cationic disorder was confirmed to be an origin for nonuniform broadening of the diffraction reflections of the hematite and corundum structures.[33,34]

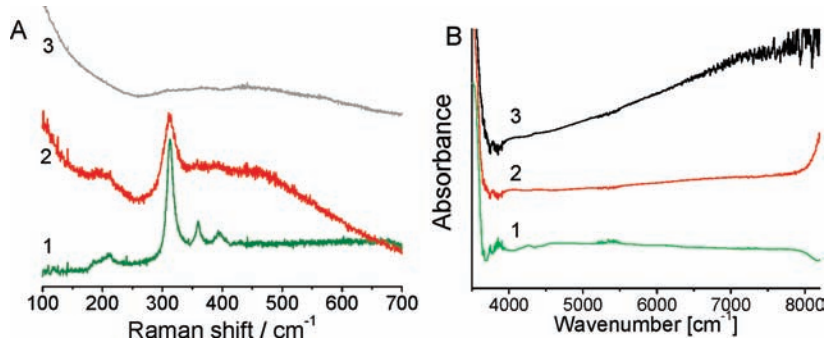

Figure 7. (A) Raman and (B) FTIR spectra of (1) white, (2) red, and (3) black c-In(OH)$_3$ at ambient pressure. In (A), the band at 309 cm^{-1} is attributed to the ν_3 In−O symmetric stretching vibration, and the bands at 356 and 391 cm^{-1} are due to the ν_3 In−O antisymmetric stretching vibrations.[30]

As indicated above, the broadening of the reflections observed in our experiments is most probably due to the partial disordering (amorphization) of the crystal structure of indium hydroxide. Pressure-induced amorphization has been documented for a wide variety of crystalline materials. The detailed mechanism responsible for pressure-induced (or strain-induced) amorphization remains elusive, however, and more than one type of transition may be involved, depending on the initial crystal structure and its stress history. For example, crystalline $Ca(OH)_2$ is transformed into a glass at room temperature under high-pressure conditions (in a DAC between 10.7 and 15.4 GPa) because of the amorphization of the Ca sublattice in $Ca(OH)_2$.[35]

The relaxation of the indium sublattice, which is highly disordered, causes localized stress gradients during rapid decompression. The magnitude of this effect is so large that it results in indium hydroxide decomposition and nucleation of metallic indium. The appearance of the (011) diffraction reflection of t-In as a shoulder of the broad, In-related (220) reflection of c-$In(OH)_3$ points out the similarity in the distances and topologies of not only these planes but also the two structures. Indeed, the mean In−In distances in the compressed c-$In(OH)_3$ were ~3.58 Å (as calculated from d_{220}), which is comparable to those in t-In (i.e., 3.29 and 3.38 Å from Rietveld refinement) and much smaller than those in the initial c-$In(OH)_3$ (i.e., 3.98 Å). As the two structures $Im\bar{3}$ [i.e., c-$In(OH)_3$] and $I4/mmm$ (i.e., t-In) have a common supergroup, $Pm\bar{3}$ (No. 200),[36,37] the transition between them can occur through a multistage diffusionless transformation path.[38] Such short pathways are particularly suitable for transitions under high pressure, as indeed is observed for the c-$In(OH)_3$ → t-In decomposition. The latter occurs as a reconstructive phase transition with considerable volume changes and atomic rearrangements.

Conclusions

In summary, a partial decomposition of indium hydroxide into metallic indium induced by a static pressure at ambient temperature has been observed. This unique process is initiated by rapid decompression, is irreversible, and seems to be intimately related to the disordering of the indium sublattice in indium hydroxide. The instability of c-$In(OH)_3$ as well as of any other metal hydroxide/oxohydroxide toward decomposition under high pressure conditions has not been reported previously.

Acknowledgment. The experiments were performed within the framework of Project "Indium Oxide (In_2O_3) under High Pressure: Rational Design of New Polymorphs and Characterization of Their Physico-Chemical Properties" of the DFG Priority Programme 1236 "Oxides, Carbides, and Nitrides at Extremely High Pressures and Temperatures" (SPP 1236). The financial support by DESY (Hamburg, Germany; Proposal I-20080181) and ESRF (Grenoble, France) is gratefully acknowledged.

JA104278P

(31) Nagarajan, L.; De Souza, R. A.; Samuelis, D.; Valov, I.; Borger, A.; Janek, J.; Becker, K. D.; Schmidt, P. C.; Martin, M. *Nat. Mater.* **2008**, *7*, 391.
(32) *International Tables for Crystallography, Volume A: Space-Group Symmetry*; Hahn, T., Ed.; International Union of Crystallography: Chester, England, 2005.
(33) Loffler, L.; Mader, W. *J. Eur. Ceram. Soc.* **2005**, *25*, 639.
(34) Loffler, L.; Mader, W. *J. Eur. Ceram. Soc.* **2006**, *26*, 131.
(35) Meade, C.; Jeanloz, R. *Geophys. Res. Lett.* **1990**, *17*, 1157.
(36) Bock, O.; Muller, U. *Z. Anorg. Allg. Chem.* **2002**, *628*, 987.
(37) Bock, O.; Muller, U. *Acta Crystallogr., Sect. B* **2002**, *58*, 594.
(38) Christy, A. G. *Acta Crystallogr., Sect. B* **1993**, *49*, 987.